Journal of Catalysis 281 (2011) 169–176

Contents lists available at ScienceDirect

Journal of Catalysis

journal homepage: www.elsevier.com/locate/jcat

Methanol oxidation on VSiBEA zeolites: Influence of V content on the catalytic properties

Maciej Trejda [a,*], Maria Ziolek [a], Yannick Millot [b,c], Karolina Chalupka [b,c], Michel Che [b,c,d], Stanislaw Dzwigaj [b,c,*]

[a] Faculty of Chemistry, A. Mickiewicz University, Grunwaldzka 6, 60-780 Poznan, Poland
[b] Laboratoire de Réactivité de Surface, UPMC Univ Paris 6, 4 Place Jussieu, 75252 Paris Cedex 05, France
[c] Laboratoire de Réactivité de Surface, CNRS, UMR 7197, 4 Place Jussieu, 75252 Paris Cedex 05, France
[d] Institut Universitaire de France, 103 Bd. Saint-Michel, 75005 Paris, France

ARTICLE INFO

Article history:
Received 7 December 2010
Revised 16 April 2011
Accepted 21 April 2011
Available online 23 May 2011

Keywords:
BEA
Zeolite
Vanadium
Methanol
Oxidation

ABSTRACT

This study deals with the influence of V content on the catalytic properties of V_xSiBEA zeolites in the oxidation of methanol. The samples are prepared following a postsynthesis method reported earlier (S. Dzwigaj, M.J. Peltre, P. Massiani, A. Davidson, M. Che, T. Sen, S. Sivasanker, Chem. Commun. (1998) 87). The incorporation of isolated mononuclear V(V) into the framework of SiBEA is evidenced by XRD, FTIR, diffuse reflectance UV–vis and NMR. It is found that, for low V content, V(V) ions are in pseudo-tetrahedral coordination *only*, either in nonhydroxylated $(SiO)_3V{=}O$ or hydroxylated $(SiO)_2(OH)V{=}O$ species in framework position. For higher V content, additional species appear in extraframework position with vanadium in octahedral coordination. FTIR investigations of pyridine adsorption show that strong Brønsted and Lewis acidic centres are present in SiBEA leading to dimethyl ether *only*, in methanol oxidation.

Upon incorporation of vanadium into the BEA framework, Lewis acidic (V^{5+}) and basic (O^{2-}) centres are generated with simultaneous appearance of partial oxidation products mainly, whose total concentration increases with vanadium content. These results suggest that those centres are responsible for the oxidation activity of V_xSiBEA zeolites. The selectivity toward formaldehyde increases with the amount of vanadium present as pseudo-tetrahedral hydroxylated $(SiO)_2(HO)V{=}O$ species. This selectivity is suggested to be related to the moderate nucleophilicity of the basic vanadyl oxygen ($V{=}O$) of $(SiO)_2(HO)V{=}O$ species.

1. Introduction

Crystalline microporous zeolites containing transition metal ions well dispersed in the structure are important catalytic materials in reactions, such as selective oxidation, hydroxylation and selective catalytic reduction of NO_x [1–3]. Their catalytic performance strongly depends on the nature, local environment and, in particular, content of transition metal ions. We recently reported [4–9] that it is possible to control the content of vanadium in BEA zeolite by using a two-step postsynthesis method that consists, in the first step, in the creation of vacant T-atom sites with associated silanol groups by dealumination of BEA zeolite with nitric acid to form SiBEA zeolite and, in the second step, in the incorporation of vanadium into the vacant T-atom sites using aqueous NH_4VO_3 solution as precursor at low concentration and pH = 2.5.

Oxidative dehydrogenation of methanol leads mainly to formation of formaldehyde, a desirable intermediate in synthesis of different organic compounds. The first commercial production began in the end of the 19th century in Germany using Cu catalyst, which was later replaced by Ag catalyst [10]. The process was carried out at high methanol concentration of above 40% at a temperature from the range 823–1023 K. In the middle of the 20th century, a procedure was developed in which a lower methanol concentration as well as lower temperature could be applied. This effect was achieved with the iron molybdate catalyst. Industrial iron molybdate catalysts applied for methanol oxidation have been described earlier [11]. Nowadays, both catalytic systems leading to formaldehyde are used. Formaldehyde and other products are formed following mechanisms that depend on the catalyst type.

Methanol oxidation can be used as a test reaction to identify the types of active site present on catalyst surfaces [12–21]. The reaction network related to methanol oxidation [14] involves two main

* Corresponding authors. Address: Laboratoire de Réactivité de Surface, UPMC Univ Paris 6, 4 Place Jussieu, 75252 Paris Cedex 05, France (S. Dzwigaj).
E-mail addresses: tmaciej@amu.edu.pl (M. Trejda), stanislaw.dzwigaj@upmc.fr (S. Dzwigaj).

0021-9517/$ - see front matter © 2011 Elsevier Inc. All rights reserved.
doi:10.1016/j.jcat.2011.04.013

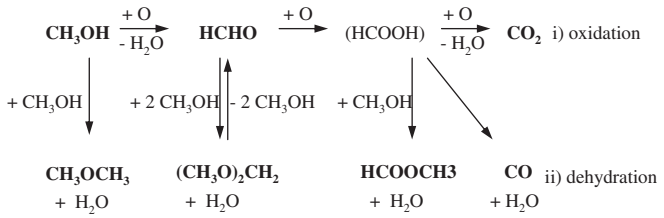

Fig. 1. Reaction network for methanol oxidation leading to various products (see text), adapted from Ref. [9].

pathways: (i) oxidation requiring oxygen (indicated by O in Fig. 1) either from the gas phase (dioxygen) or from the catalyst (mononuclear oxygen) and (ii) dehydration that does not require oxygen.

With the exception of dimethyl ether (CH_3OCH_3) directly produced by bimolecular dehydration of methanol, all other carbon-containing products (indicated in bold in Fig. 1) require at least one oxidation step.

Tatibouet has reviewed the use of methanol oxidation to probe the acido-basic character of the catalytically active sites [14]. While dimethyl ether selectivity is generally related to the acidic character of the catalyst employed and to its dehydration ability, the other products require catalyst with increasing basicity or nucleophilic character in the order:

$$CH_2O \leqslant (CH_3O)_2CH_2 < HCOOCH_3 < CO,\ CO_2$$

On the basis of the product favoured, three main types of character can be distinguished: highly acidic (dimethyl ether), highly basic (carbon oxides) and bifunctional acid–base (mild oxidation products). From this picture, selectivity appears to be the key parameter to evaluate the acid–base properties of the catalyst.

Practically, the products observed depend on the catalyst nature, reaction temperature and contact time (both influencing conversion) as well as reactant partial pressure. For instance, an increase in conversion favours consecutive reactions, leading at high conversion predominantly to the formation of CO_2, the most thermodynamically favoured product.

Vanadium-based species exhibit significant activity in methanol oxidation [12,14,16]. Moreover, the environment of active sites strongly affects activity and selectivity [14,15]. The high selectivity toward formaldehyde is observed when the nucleophilicity of oxygen present in the neighbourhood of vanadium is moderate [15]. The increase in nucleophilicity in the surrounding of vanadium species leads to the stronger chemisorption of formaldehyde and the formation of methylal, which can be transformed into methyl formate by further reaction with CH_3OH. Further increase in nucleophilicity causes the total oxidation of methanol.

This paper deals with the influence of vanadium content on the catalytic properties of V_xSiBEA zeolites in methanol oxidation as evidenced by XRD, FTIR, ^{29}Si MAS NMR, ^{1}H–^{29}Si CP MAS NMR, ^{1}H MAS NMR, DR UV–vis, ^{51}V MAS NMR and catalysis data. To the best of our knowledge, this is the first report on the oxidation of methanol catalysed by vanadium incorporated into the framework of BEA zeolite by the two-step postsynthesis method described above and reported earlier [4].

2. Experimental

2.1. Materials

A tetraethylammonium BEA zeolite (TEABEA) (Si/Al = 11) provided by RIPP (China) was treated with a 13 N HNO3 solution (4 h, 353 K) under stirring to obtain a dealuminated BEA (Si/Al = 1000) noted thereafter SiBEA, which was separated by centrifugation, washed with distilled water and finally dried in air overnight at 353 K.

The SiBEA solid was then contacted with an aqueous solution of ammonium metavanadate (NH_4VO_3) in excess (2 g zeolite in 20 ml of solution) and with a concentration varying from 0.25×10^{-2} to 9×10^{-2} mol L^{-1}. Because of its low concentration at pH = 2.5, the aqueous solution is expected to mainly contain monomeric VO_2^+ ions [22]. The suspension was left for 3 days at room temperature without any stirring. The solids obtained were recovered by centrifugation and dried at 353 K overnight. The samples were labelled V_xSiBEA with x = 0.3, 0.7, 2.05 and 4.7 V wt.%.

2.2. Techniques

Powder X-ray diffractograms (XRD) were recorded with a Siemens D5000 apparatus using the Cu Kα radiation (λ = 154.05 pm).

Infrared spectra were registered with a Bruker Vector 22 FTIR spectrometer. Samples were pressed at ~0.2 tons cm^{-2} into thin wafers of ca. 10 mg cm^{-2} and placed inside the IR cell. Catalysts were outgassed at 673 K for 3 h and then contacted with pyridine (PY) at 423 K for 0.5 h. After saturation with PY, the samples were outgassed at 423, 473, 523 and 573 K for 0.5 h at each temperature. Spectra were recorded at room temperature in the range 4000–400 cm^{-1}. The spectrum of the IR cell without any sample ("background spectrum") was subtracted from all recorded spectra. The IR spectra of the activated samples (after outgassing at 673 K) were subtracted from those recorded after adsorption of PY.

^{29}Si NMR spectra of samples, transferred at ambient atmosphere into 7 mm zirconia rotors, were recorded with a Bruker Avance spectrometer at 99.4 MHz, some in cross-polarization (CP) mode (^{29}Si CP MAS NMR). The chemical shifts of silicon were measured with reference to tetramethylsilane (TMS). ^{29}Si MAS NMR spectra were obtained at 5 kHz spinning speed, 2.5 μs excitation pulse and 10 s recycle delay. 3-(Trimethylsilyl)-1-propanosulphonic sodium salt was used for setting the Hartmann–Hahn condition. The proton $\pi/2$ pulse duration, the contact time and recycle delay were 6.8 μs, 5 ms and 5 s, respectively.

^{1}H MAS NMR spectra were recorded at 500 MHz with a 90° pulse duration of 3 μs and a recycle delay of 5 s. To record only the proton signal of the sample, the equipment for rotation (12 kHz) was carefully cleaned with ethanol and dried in air at room temperature. The proton signals from probe and rotor were subtracted from the total free induction decay.

DR UV–vis spectra were recorded at ambient atmosphere on a Cary 5000 Varian spectrometer equipped with a double integrator with polytetrafluoroethylene as reference.

^{51}V NMR spectra were recorded with a Bruker Avance 500 spectrometer at 131.6 MHz and with a 2.5-mm zirconia rotor spinning at 35 kHz. The spectra were acquired with 0.5-s recycle delay and pulse duration of 3.5 μs. Chemical shifts of vanadium were measured with reference to NH_4VO_3 (δ = −570 ppm).

2.3. Methanol oxidation

The reaction was performed in a fixed-bed flow reactor on 0.04 g of pressed catalyst (particles with 0.5–1 mm diameter). The sample was activated in flowing He (40 cm^3 min^{-1}) at 673 K for 2 h and then cooled to 523 K, the reaction temperature. A gas mixture of MeOH and O_2 (MeOH/O_2 molar ratio = 2), diluted with He as carrier gas, was used with a total flow rate of 40 cm^3 min^{-1}. The reaction products were analysed by gas chromatography (GC 8000 Top) equipped with flame ionization (FID) and thermal conductivity (TCD) detectors. Reactants and products were separated on a 60 m DB-1 column filled with dimethylpolysiloxane kept at 313 K.

3. Results and discussion

3.1. Incorporation of vanadium into the framework of dealuminated BEA

3.1.1. X-ray diffraction

Incorporating vanadium into SiBEA leads to an increase of the d_{302} spacing (results not shown) from 3.912 (SiBEA) to 3.941 Å ($V_{2.05}$SiBEA), indicating some expansion of the BEA structure and confirming incorporation of vanadium into the framework, in line with earlier conclusions for VSiBEA zeolites [4–7].

The absence of diffraction lines due to extraframework compounds in V_xSiBEA indicates a good dispersion of vanadium. It is important to note that the surface area (655 $m^2\,g^{-1}$) and the micropore volume (0.24 $cm^3\,g^{-1}$) of SiBEA do not change after incorporation of vanadium, suggesting that the latter does not sensibly affect the zeolite porosity.

3.1.2. FT-IR

As shown earlier [4,6], the FT-IR spectrum of TEABEA zeolite calcined at 823 K for 15 h exhibits five IR bands due to the OH stretching modes of AlOH groups at 3781 and 3665 cm^{-1}, Si—O(H)—Al groups at 3609 cm^{-1}, isolated SiOH groups at 3740 cm^{-1} and H-bonded SiOH groups at 3520 cm^{-1}.

The treatment of TEABEA zeolite by aqueous HNO_3 solution leads to the removal of framework Al atoms, as evidenced by the disappearance of bands at 3781 and 3665 (AlOH groups) and 3609 cm^{-1} (Si—O(H)—Al groups), as shown earlier for VSiBEA zeolite [4–6]. The appearance of narrow bands at 3736 and 3710 cm^{-1} related to isolated internal and terminal silanol groups and of a broad band at 3520 cm^{-1} due to H-bonded SiOH groups in SiBEA reveals the presence of vacant T-atom sites associated with silanol groups, in line with earlier data for VSiBEA zeolite [4–6].

The impregnation of SiBEA by aqueous NH_4VO_3 solution reduces the intensity of the latter bands, particularly that at 3520 cm^{-1} due to H-bonded SiOH groups (Fig. 2), suggesting that silanol groups react with the vanadium precursor to form stable nonhydroxylated framework pseudo-tetrahedral $(SiO)_3V{=}O$ species, in line with earlier work on BEA zeolite [5,23]. Simultaneously, two FTIR bands at 3645 and 3620 cm^{-1} appear which are assigned to the hydroxyl vibration of $(SiO)_2(HO)V{=}O$ species located at two different crystallographic sites, in line with earlier data for VSiBEA zeolite [7,23]. Those V species are in much lower amount than nonhydroxylated $(SiO)_3V{=}O$ species, confirming earlier data on VSiBEA zeolite [5,6,23].

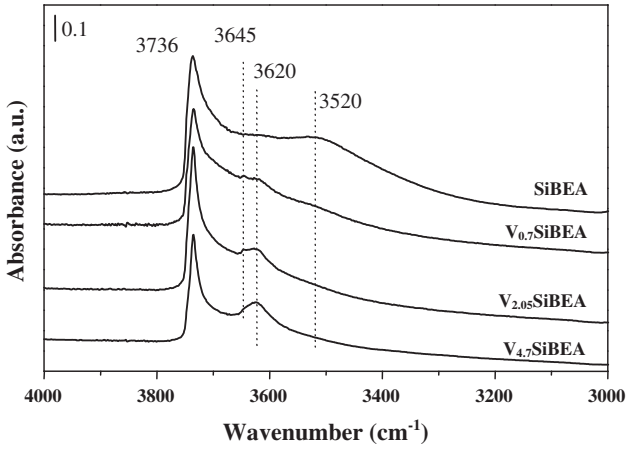

Fig. 2. FTIR spectra recorded at room temperature of SiBEA, $V_{0.7}$SiBEA, $V_{2.05}$SiBEA and $V_{4.7}$SiBEA outgassed at 673 K for 3 h (10^{-3} Pa) in the vibrational range of OH groups.

The structure of the $(SiO)_2(HO)V{=}O$ species with the wavenumbers of its associated vibrators can now be refined (Fig. 3), on the basis of the above results (SiO–H at 3620 and 3645 cm^{-1}) and earlier data obtained by photoluminescence (V=O at 1018 cm^{-1}, referred to as species α with structure A) [5], theoretical calculations [23] and IR and photoacoustic spectroscopies (Si—OV at 980 and Si—OH at 950 cm^{-1}) [6].

The acidic sites in SiBEA and V_xSiBEA were probed by means of pyridine adsorption (see Section 2), and Fig. 4 gives the corresponding IR spectra.

For SiBEA, two bands typical of pyridinium cations are observed at 1545 and 1638 cm^{-1}, indicating the presence of Brønsted acidic centres (most likely related to the acidic proton of Al–O(H)–Si groups, present as traces after the dealumination step). The bands at 1454 and 1622 cm^{-1} correspond to pyridine interacting with strong Lewis acidic centres (Al^{3+}) and those at 1445 and 1596 cm^{-1} (Fig. 4) to pyridine interacting with weak Lewis acidic centres (hydroxyls) and/or pyridine physisorbed, in line with earlier data for BEA [6].

The introduction of vanadium leading to V_xSiBEA generates bands at 1449 and 1608 cm^{-1} corresponding to pyridine adsorbed on Lewis acidic centres (V^{5+}). The bands at 1545 and 1638 cm^{-1} observed for both V_xSiBEA and SiBEA indicate a similar strength of Brønsted acidic centres. In contrast, for V_xSiBEA, new Lewis acidic centres exhibit a lower strength than that of centres present on SiBEA, as shown by the position of the bands (1608 *vs.* 1622 cm^{-1}). These bands disappear upon outgassing at increasing temperature (Table 1) as discussed below. As reported earlier for BEA zeolite [6], the Brønsted acidic centres evidenced in V_xSiBEA are related to the acidic proton of OH group of framework hydroxylated $(SiO)_2(HO)V{=}O$ species as deduced from their disappearance upon adsorption of pyridine (results not shown). However, as reported earlier for BEA and sodalite systems, only a small part of all framework tetrahedral V(V) ions appears as such species [23].

The number of acidic centres calculated from the amount of pyridine outgassed at 473 K for 0.5 h is given in Table 1. One can notice that the number of Lewis acidic centres increases with the vanadium content (0.3, 0.7 and 2.05 wt.%) with some saturation for 4.7 wt.% ($V_{4.7}$SiBEA), suggesting that not all vanadium ions are accessible for pyridine, as in the case of vanadium oxide clusters. The number of Brønsted acidic centres increases with vanadium content to reach a maximum for 2.05 wt.%, before decreasing for $V_{4.7}$SiBEA.

Table 1 also gives the total number of acidic centres determined from the amount of pyridine remaining adsorbed after outgassing the samples at 473, 523 and 573 K, making it possible to estimate the acid strength. There is a large difference in the acid strength between SiBEA and V_xSiBEA. For SiBEA, outgassing at 573 K leads to a decrease of ca. 20% of acidic centres compared to the situation after outgassing at 473 K, whereas for $V_{0.3}$SiBEA, this decrease is ca. 85%. Thus, the acid strength of SiBEA appears to decrease after a

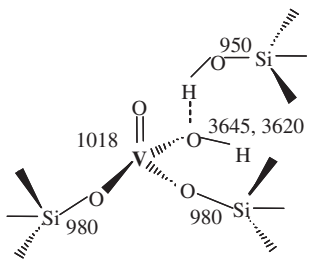

Fig. 3. Schematic representation of the hydroxylated $(SiO)_2(HO)V{=}O$ species hydrogen bonded to a neighbouring SiOH group, with the wavenumbers (cm^{-1}) of the associated vibrators.

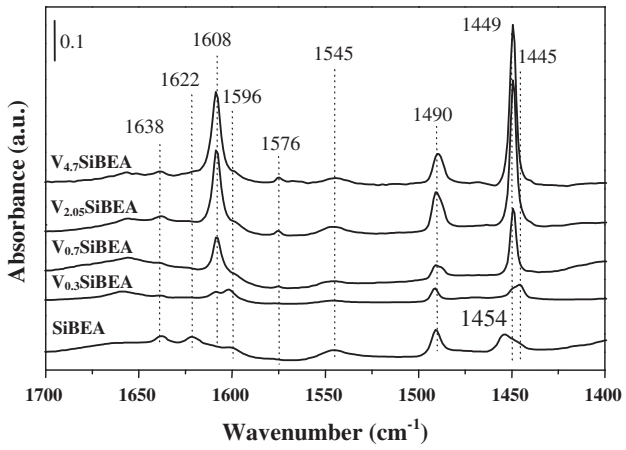

Fig. 4. FTIR spectra recorded at room temperature after adsorption of pyridine at 423 K followed by desorption at 473 K for 0.5 h of SiBEA, $V_{0.3}$SiBEA, $V_{0.7}$SiBEA, $V_{2.05}$SiBEA and $V_{4.7}$SiBEA.

Table 1
Number of acidic centres of V_xSiBEA zeolites determined from the amount of pyridine remaining adsorbed after outgassing the samples at 473 K (number of Lewis or Brønsted acidic centres), and 473, 523 and 573 K (total number of acidic centres).

Sample	Lewis acidic centres ($\times10^{17}$)	Brønsted acidic centres ($\times10^{17}$)	Total number of acidic centres ($\times10^{17}$)		
			Pyridine 473 K	Desorption 523 K	Temperature 573 K
SiBEA	17.8	7.4	25.2	22.4	20.1
$V_{0.3}$SiBEA	15.0	2.1	17.1	7.0	2.8
$V_{0.7}$SiBEA	71.7	3.8	75.5	62.2	30
$V_{2.05}$SiBEA	160.2	6.8	167.0	115.6	57.9
$V_{4.7}$SiBEA	176.9	5.4	182.3	100.3	34.6

small amount of vanadium is incorporated (compare spectra a and b of Fig. 4). These results evidence the role of the surroundings of acidic centres on their strength.

3.1.3. 29Si MAS NMR and ^1H—^{29}Si CP MAS NMR

The ^{29}Si MAS NMR spectrum of SiBEA (Fig. 5) shows three peaks at −102.5, −111.1 and −114.2 ppm. The latter two peaks are due to framework Si atoms in a $Si(OSi)_4$ environment, located at different crystallographic sites, in line with earlier data for BEA system [8]. The broad peak at −102.5 ppm corresponds to Si atoms in a $Si(OH)(OSi)_3$ environment, as reported earlier for BEA zeolite [24], in line with the removal of nearly all Al atoms upon dealumination, leading to a ratio Si/Al = 1000.

This is confirmed by the increased intensity of the −102.5 ppm peak in the NMR spectrum in CP mode (Fig. 6), which enhances the signal of ^{29}Si nuclei close to protons, as in the case of the $Si(OH)(OSi)_3$ species. Moreover, a small amount of Si atoms in a $Si(OH)_2(OSi)_2$ environment is evidenced by the very weak peak at about −92.2 ppm. The peak at −111.1, with a shoulder at −114.2 ppm, appears to be due to framework Si atoms in a $Si(OSi)_4$ environment, located at different crystallographic sites, in line with earlier data for BEA zeolite [8].

After incorporation of increasing amount of V into SiBEA, the intensity of the peak at around −(102.0–103.8) ppm is reduced (Fig. 5), confirming the reaction between NH_4VO_3 and SiOH groups. It is important to note that up to four H-bonded SiOH groups may be consumed by each V ion incorporated into a vacant T-atom site. This is confirmed by the CP spectra of $V_{0.3}$SiBEA, $V_{0.7}$SiBEA and $V_{2.05}$SiBEA (Fig. 6), which show that the peak at about −(102.0–103.8) ppm

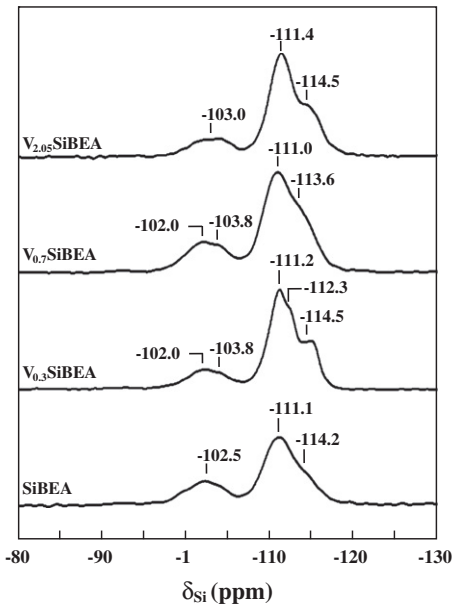

Fig. 5. ^{29}Si MAS NMR spectra recorded at room temperature of SiBEA, $V_{0.3}$SiBEA, $V_{0.7}$SiBEA and $V_{2.05}$SiBEA as prepared in 7 mm (external diameter) zirconia rotors.

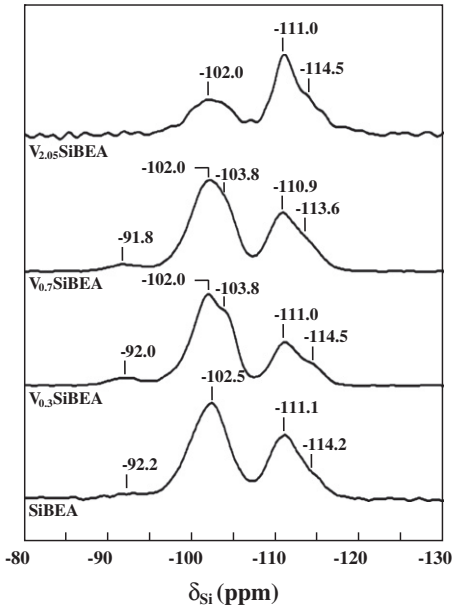

Fig. 6. ^{1}H—^{29}Si CP MAS NMR spectra recorded at room temperature of SiBEA, $V_{0.3}$SiBEA, $V_{0.7}$SiBEA and $V_{2.05}$SiBEA as prepared in 7 mm (external diameter) zirconia rotors.

corresponding to Si atoms in the $Si(OH)(OSi)_3$ environment is smaller for $V_{2.05}$SiBEA than that observed at −102.5 ppm for SiBEA (Fig. 6). Moreover, the doublet observed at around −(102.0–103.8) ppm for $V_{0.3}$SiBEA and $V_{0.7}$SiBEA suggests two types of surroundings of Si atoms in $Si(OH)(OSi)_3$ species.

3.1.4. ^1H MAS NMR

In the ^{1}H MAS NMR spectrum of SiBEA (Fig. 7), two main peaks are observed at 1.3 and 5.4 ppm due to isolated SiOH protons and H-bonded SiOH groups present at vacant T-atom sites, respectively, as shown earlier for different zeolites [25–29].

In addition, the small peak at 3.2–2.8 ppm is probably due to protons of H-bonded SiOH groups located in a second type of

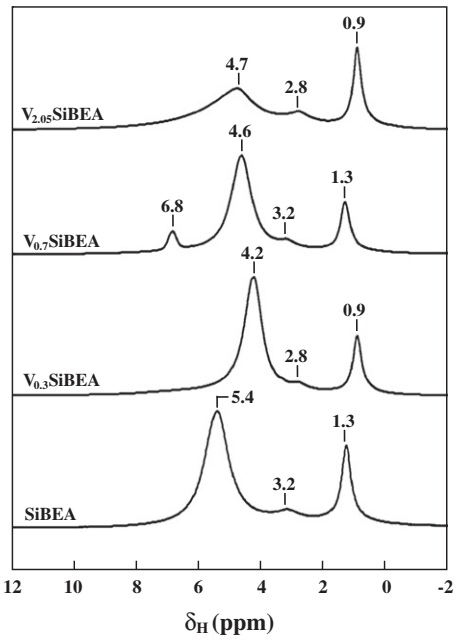

Fig. 7. ^{1}H MAS NMR spectra recorded at room temperature of SiBEA, $V_{0.3}$SiBEA, $V_{0.7}$SiBEA and $V_{2.05}$SiBEA as prepared in 4 mm (external diameter) zirconia rotors.

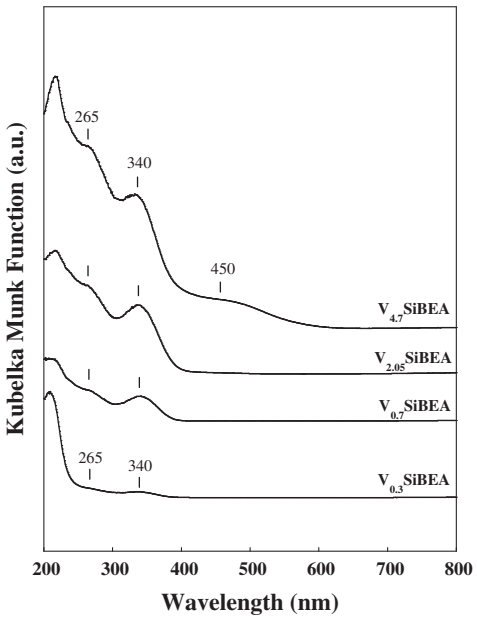

Fig. 8. DR UV–vis spectra recorded at room temperature of $V_{0.3}$SiBEA, $V_{0.7}$SiBEA, $V_{2.05}$SiBEA and $V_{4.7}$SiBEA as prepared.

crystallographic site. The similar peaks assigned to proton of isolated and H-bonded SiOH groups were observed for silicalite [28] and silica [30]. Moreover, for $V_{0.7}$SiBEA, a small peak at 6.8 ppm is observed, which is not assigned yet. The disappearance of the peaks at 5.4, 3.2 and 1.3 ppm upon incorporation of V atoms in SiBEA (Fig. 7) evidences the reaction of the NH_4VO_3 precursor with H-bonded and isolated SiOH groups. The spectra of $V_{0.3}$SiBEA, $V_{0.7}$SiBEA and $V_{2.05}$SiBEA exhibit a peak observed at 4.2, 4.6 and 4.7 ppm, respectively, which could be assigned to H-bonded SiOH groups still present in the samples and not consumed by reaction with the NH_4VO_3 precursor.

3.2. Characterization of the coordination of vanadium

3.2.1. DR UV–visible

The DR UV–visible spectra of V_xSiBEA (Fig. 8) do not show any d–d band expected for V^{IV} ($3d^1$) ions [31,32] in the range 600–800 nm.

For $V_{0.3}$SiBEA and $V_{0.7}$SiBEA, two broad bands are observed at 265 and 340 nm (Fig. 8), which are assigned to oxygen–tetrahedral V(V) charge transfer (CT) transitions, involving bridging (V—O—Si) and terminal (V=O) oxygens, respectively, to form pseudo-tetrahedral $(SiO)_3V{=}O$ species in line with earlier work on VBEA and VFMI zeolites [5,33]. These species correspond to V(V) framework ions [6,9].

Similar bands are observed at higher V content (2.05 and 4.7 wt.%), but in addition, a band appears near 450 nm, due to a low-energy CT transition involving octahedral V(V) ions, in line with earlier work on VBEA and VFMI zeolites [4,6,33]. These octahedral V(V) ions belong to extraframework species [6,9].

3.2.2. ^{51}V MAS NMR

The presence of pseudo-tetrahedral $(SiO)_3V{=}O$ species can be confirmed by NMR via the peak at −620 ppm (Fig. 9) corresponding to one kind of V(V) in line with earlier data for various materials with isolated V(V) in distorted tetrahedral symmetry [33–37].

In contrast, for $V_{4.7}$SiBEA, two additional small peaks are observed at −505 and −535 ppm probably related to the presence

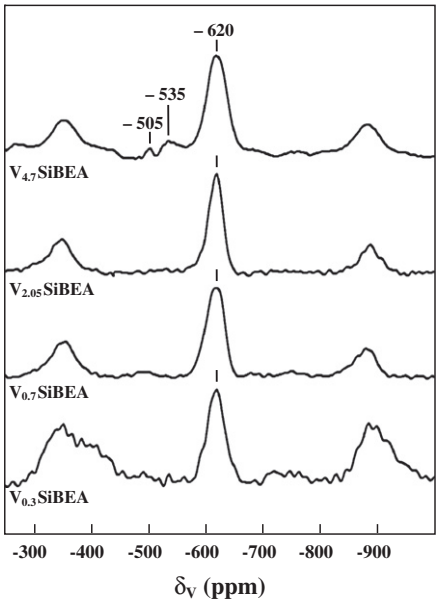

Fig. 9. ^{51}V MAS NMR spectra recorded at room temperature of $V_{0.3}$SiBEA, $V_{0.7}$SiBEA, $V_{2.05}$SiBEA and $V_{4.7}$SiBEA as prepared.

of distorted octahedral V species, in line with earlier work on VMCM-41 mesoporous materials [36].

In conclusion, the above DR UV–vis and ^{51}V MAS NMR results suggest that for V_xSiBEA zeolites at low content (x = 0.3 and 0.7 wt.%), vanadium is found to be as V(V) in $(SiO)_3V{=}O$ and $(SiO)_2(HO)V{=}O$ species in pseudo-tetrahedral coordination *only* and at higher content (x = 2.05 and 4.7 wt.%) as V(V) in both pseudo-tetrahedral and octahedral coordinations, the latter corresponding to extraframework species.

3.3. Oxidation of methanol

As reviewed earlier [14], acidic and basic centres are involved in the oxidation of methanol by oxide catalysts. Although hydrogen

abstraction from methanol to form $\cdot CH_2OH$ radicals has been shown by EPR to occur at 190–210 K on adsorbed O^- on Mo grafted to silica [37], it is admitted that, at the reaction temperature generally used (ca. 523 K), the first step that also involves the abstraction of hydrogen leads rather to methoxy species [14].

In the case of V_xSiBEA zeolites, nonhydroxylated $(SiO)_3V{=}O$ and hydroxylated $(SiO)_2(HO)V{=}O$ species can be considered as either redox or Lewis (V^{5+}) and Brønsted acidic (proton of the OH group) and basic (O^{2-}) centres on which hydrogen abstraction can take place:

$$(SiO)_3V{=}O + CH_3OH \rightarrow (SiO)_3(CH_3O)VOH \quad (1)$$

$$(SiO)_2(HO)V{=}O + CH_3OH \rightarrow (SiO)_2(CH_3O)V{=}O + H_2O \quad (2)$$

Further transformation of the methoxy species depends on the kind and strength of active centres [38]. The presence of strong acidic centres and the absence of basic centres in the neighbourhood of methoxy species may cause its interaction with a second CH_3OH molecule to form dimethyl ether.

Table 2 gives the conversion and selectivity for methanol oxidation in steady-state conditions at 523 K on SiBEA and V_xSiBEA zeolites.

The highest conversion (11.2%) is observed for SiBEA, and the *only* product is dimethyl ether, confirming the acidic character of SiBEA. A similar behaviour has been evidenced for acidic Mo-based polyoxometallates [39,40]. The IR data on pyridine adsorption (Fig. 4 and Table 1) show that SiBEA has the highest number of Brønsted acidic centres, in line with the highest conversion. It appears that the absence of vanadium species and basic centres in SiBEA results in the lack of oxidation products.

The presence of a small amount of vanadium in SiBEA leads to a significant decrease in methanol conversion (Table 2) with a simultaneous shift toward partial oxidation products typical of the redox character of V_xSiBEA zeolites. The selectivity to dimethyl ether decreases from 100% for SiBEA to 55% for the $V_{0.3}$SiBEA sample, in agreement with its weak acidity (Table 1). Noteworthy, the total oxidation to CO_2 that requires the presence of basic centres becomes significant on $V_{0.3}$SiBEA zeolite.

The increase in V content in V_xSiBEA leads to (Table 2): (i) a decrease in selectivity toward CO_2 caused by the competition between the participation of basic centres to total oxidation and the transformation of methoxy species into formaldehyde and (ii) an increase in the selectivity toward formaldehyde or partial oxidation products.

Formaldehyde chemisorbed on acidic centres can desorb as such or be further transformed to formate species [38]. The latter process involves the reduction of V(V) to V(IV) (confirmed by EPR investigation, results not shown); thus, vanadium can be considered as redox site [19]. It is important to stress that the presence of basic oxygen in the neighbourhood of vanadium species is required to transform methoxy species into formaldehyde by hydrogen abstraction. This oxygen is also involved in the redox cycle of vanadium in the further transformation of chemisorbed formaldehyde into partial oxidation products (e.g. methyl formate). The reaction pathway depends on the strength of acidic centres. The lower their strength, the easier the desorption of formaldehyde. Pyridine adsorption data show that the number of weak Lewis acidic centres increases with vanadium content while the number of Brønsted acidic centres reaches a maximum for 2.05 V wt.% (Table 1).

The incorporation of vanadium into SiBEA generates both weak Lewis acidic centres and basic oxygen centres as shown by the increase in the number of Lewis acidic centres (Table 1) and in the intensity of the UV–vis band at 340 nm (attributed to charge transfer between oxygen and tetrahedral V(V) in $(SiO)_3V{=}O$ and $(SiO)_2(HO)V{=}O$ species, the latter being evidenced by IR (Fig. 8)), respectively.

The basic vanadyl oxygen of $(SiO)_3V{=}O$ and $(SiO)_2(HO)V{=}O$ species is able to abstract hydrogen from methoxy groups to form formaldehyde as suggested from DFT calculations performed for methanol oxidation on silica-supported vanadia and other oxides [15]. Formaldehyde can be obtained on V_xSiBEA zeolite as a result of H transfer from methoxy groups to the basic vanadyl oxygen of both $(SiO)_3V{=}O$ and $(SiO)_2(HO)V{=}O$ species (Eqs. (1) and (2)). However, because of the high nucleophilicity of the basic vanadyl oxygen, $(SiO)_3V{=}O$ species can strongly chemisorb formaldehyde and lead to its full oxidation to CO_2. In contrast, on the less nucleophilic basic vanadyl oxygen of $(SiO)_2(HO)V{=}O$ species, formaldehyde being less strongly chemisorbed can desorb. As shown earlier for BEA and sodalite systems [23], the very few pseudo-tetrahedral V(V) ions present in V_xSiBEA as hydroxylated $(SiO)_2(HO)V{=}O$ species probably explain the very low methanol conversion (<6%) and low selectivity toward formaldehyde, in particular, for low V content (<40%).

As mentioned earlier, the proton of framework $(SiO)_2(OH)V{=}O$ species is likely to be responsible for the Brønsted acidity of V_xSiBEA zeolites. The methoxy species formed on Lewis (Eq. (1)) or Brønsted (Eq. (2)) acidic centres can react further with CH_3OH molecule to form dimethyl ether or can be transformed into formaldehyde in the presence of basic centres that abstract hydrogen. The low selectivity (below 50%) toward formaldehyde for lower V content (<2.05 wt.%) (Table 2) can be due to the low concentration of basic vanadyl oxygen of $(SiO)_2(OH)V{=}O$ species in V_xSiBEA (Fig. 3), in line with earlier data on BEA and sodalite system [23]. On the other hand, the presence of excess CH_3OH at low conversion causes its reaction with methoxy species to form dimethyl ether.

Increasing the vanadium content influences both conversion and selectivity: (i) the conversion linearly increases (Fig. 10) and (ii) the selectivity toward formaldehyde steadily increases while that toward dimethyl ether decreases (Fig. 11). One can also observe a linear increase in selectivity toward formaldehyde with the total number of acidic centres (Fig. 12).

For $V_{0.3}$SiBEA and $V_{0.7}$SiBEA with a low amount of acidic centres, the formation of dimethyl ether slightly increases. With a subse-

Table 2
Conversion and selectivity determined at 523 K for methanol oxidation on V_xSiBEA zeolites.

Catalyst	Time[a] (min)	Methanol conversion[b] (%)	Selectivity[b] (%)					
			$(CH_3)_2O$	HCHO	$(CH_3O)_2CH_2$	$HCOOCH_3$	$\sum S^c$	CO_2
SiBEA	70	11.2	100	–	–	–	–	–
$V_{0.3}$BEA	130	1.1	55	16	4	5	25	20
$V_{0.7}$BEA	70	1.3	59	35	5	–	40	1
$V_{2.05}$BEA	70	2.4	24	56	11	7	74	2
$V_{4.7}$BEA	70	5.4	19	63	8	9	80	1

[a] Time expressed in minutes (min) after which the steady state is reached.
[b] The data correspond to the steady state.
[c] ΣS represents the sum of the selectivities toward partial oxidation products.

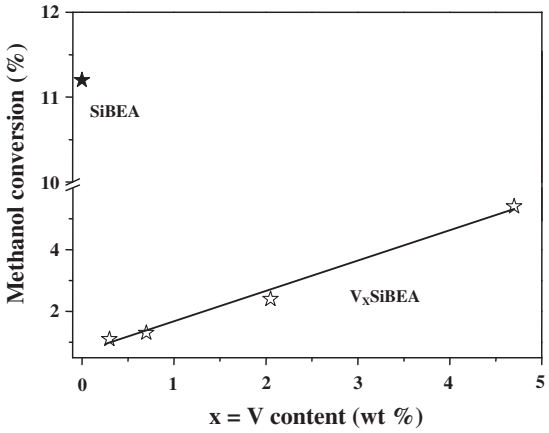

Fig. 10. Conversion of methanol at 523 K plotted as a function of vanadium content.

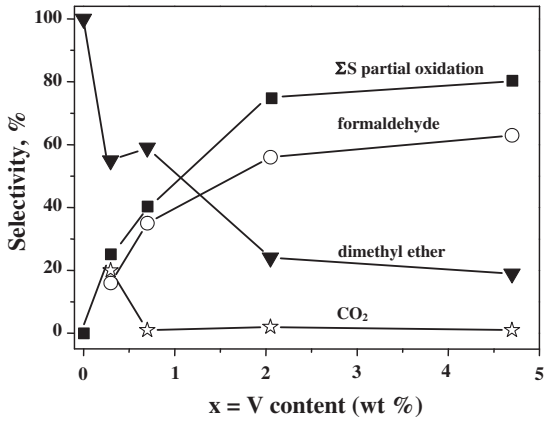

Fig. 11. Product selectivity in methanol oxidation at 523 K plotted as a function of vanadium content. $\sum S$ represents the sum of the selectivities toward partial oxidation products.

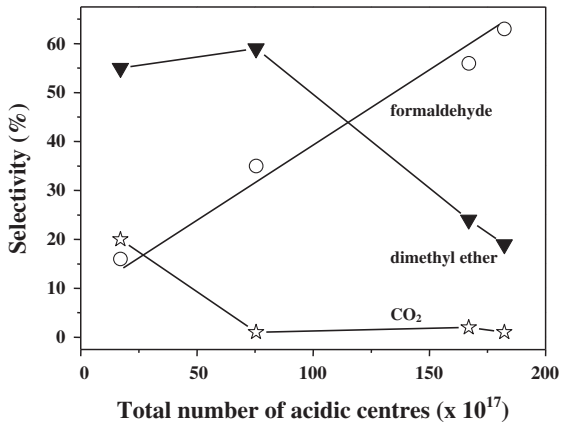

Fig. 12. Product selectivity in methanol oxidation at 523 K plotted as a function of total number of acidic centres.

quent increase in the number of acidic centres, the redox products start to dominate. The highest selectivity toward formaldehyde is observed for $V_{4.7}$SiBEA, which exhibits the highest amount of hydroxylated $(SiO)_2(HO)V{=}O$ species evidenced by the most intense bands at 3620 and 3645 cm^{-1} among V_xSiBEA samples (Fig. 2).

The decrease of dimethyl ether and CO_2 selectivities and the increase of formaldehyde selectivity with increasing vanadium content clearly evidence that the presence of hydroxylated $(SiO)_2(HO)V{=}O$ species (Fig. 3) favours the oxidation to formaldehyde.

There is some similarity, for methanol oxidation, in the behaviour of the two series of catalysts, such as V_xSiBEA zeolites (x = 0.3, 0.7, 2.05 and 4.7 V wt.%) and $H_{3+n}PV_nMo_{12-n}O_{40}$ (n = 0, 1, 2, 3) heteropolyacids [41,42], where vanadium is incorporated into the two types of structure, SiBEA zeolite on one side and Keggin $PMo_{12}O_{40}^{3-}$ polyoxometallate on the other. The two systems exhibit acidic and redox properties. There is however a difference: Vanadium is in pseudo-tetrahedral coordination in V_xSiBEA zeolites for low vanadium content (x = 0.3 and 0.7) and in octahedral coordination in the Keggin structure. Thus, V_xSiBEA zeolites with high vanadium content (x = 2.05 and 4.7) with both pseudo-tetrahedral and octahedral vanadium coordinations are intermediate between the two previous cases.

In both systems, zeolites and polyoxometallates, increasing the vanadium content leads to higher selectivity toward formaldehyde, by favouring oxidative dehydrogenation at the expense of dehydration, with a concomitant decrease in selectivity toward dimethyl ether. There does not seem to be a noticeable difference in the behaviour of vanadium in pseudo-tetrahedral or octahedral coordination. This may be due to the presence of water formed by dehydration and/or oxidative dehydrogenation (Fig. 1) with a subsequent change, in reaction conditions, of the coordination of vanadium from pseudo-tetrahedral to octahedral. It is known that washing with ammonium acetate removes octahedral vanadium species in extraframework position but not pseudo-tetrahedral vanadium in framework position [6]. Work is in progress to investigate the effect of such washing on the catalytic properties of V_xSiBEA zeolites in methanol oxidation.

Finally, it is noteworthy that the selectivity toward methyl formate is low, with a slight tendency to increase with vanadium content (Table 2). It has been shown earlier, for supported molybdenum oxide, that the selectivity toward methyl formate could be used as a dispersion-sensitive probe [13,43]. The mechanism of its origin involves the formation of formaldehyde from methanol on Mo sites, followed by its migration to silica, where it further reacts with methoxy groups to form methyl formate, via a hemiacetal intermediate [12,43]. The fact that both the acidic and redox part are gathered within the same $(SiO)_2(HO)V{=}O$ species might explain why such migration is not possible in the case of V_xSiBEA zeolites and why the selectivity toward methyl formate is very low. Work is being performed to document this possibility.

4. Conclusions

The goal of this work is to evidence the role of V content of V_xSiBEA zeolites in the oxidation of methanol. The incorporation of vanadium into the framework of SiBEA by a two-step postsynthesis method [4] to form V_xSiBEA zeolites (x = 0.3, 0.7, 2.05 and 4.7 V wt.%) is investigated by XRD, FTIR, ^{29}Si MAS NMR, ^{1}H—^{29}Si CP MAS NMR and ^{1}H MAS NMR.

The dealumination of BEA to form SiBEA zeolite leads to an IR band at 3520 cm^{-1} due to hydrogen-bonded SiOH groups, associated with vacant T-atom sites. The significant reduction of intensity of that band and of the NMR peak near −102.0 ppm, due to $Si(OH)(OSi)_3$ species upon impregnation of SiBEA by a solution of NH_4VO_3, suggests that the latter specifically reacts with hydrogen-bonded SiOH groups to form $(SiO)_2(HO)V{=}O$ species. Those species are identified by the two IR bands at 3645 and 3620 cm^{-1} assigned to the O—H group and corresponding to two different crystallographic sites.

IR, diffuse reflectance UV–vis and NMR data suggest that, for low content (0.3 and 0.7 wt.%), V(V) ions are found to belong to pseudo-tetrahedral nonhydroxylated $(SiO)_3V{=}O$ and hydroxylated $(SiO)_2(OH)V{=}O$ species in framework position, while, for higher content, additional species are observed with octahedral vanadium in extraframework position.

IR data on pyridine adsorption show that strong Brønsted and Lewis acidic centres are present in SiBEA (originating from traces of Al^{3+}). Upon impregnation of SiBEA with a NH_4VO_3 solution, weak Lewis acidic (V^{5+}) as well as basic (O^{2-}) centres appear as a result of the incorporation of vanadium into the BEA framework. The amount of pseudo-tetrahedral $(SiO)_2(OH)V{=}O$ species increases with V content and determines the changes in conversion and selectivity in methanol oxidation. To the best of our knowledge, this is the first time that this reaction is reported for zeolitic systems with vanadium in framework position.

Low vanadium content leads to low methanol conversion. For increasing vanadium content, the selectivity toward dimethyl ether as well as the total oxidation of methanol to CO_2 decreases while the total concentration of partial oxidation products increases.

The selectivity toward formaldehyde increases with the amount of pseudo-tetrahedral hydroxylated $(SiO)_2(HO)V{=}O$ species. It is suggested that this selectivity is related to the moderate nucleophilicity of the basic vanadyl oxygen (V=O) of this hydroxylated V species.

Further work is in progress to get more insight into the reaction mechanism and nucleophilicity of the vanadyl oxygen.

Acknowledgments

S.D. gratefully acknowledges the CNRS (France) for financing his Research position. The Polish Ministry of Science and Higher Education (Grant 118/COS/2007/03) and COST D36/0006/06 are acknowledged for financial support.

References

[1] P.B. Venuto, Micropor. Mater. 2 (1994) 297.
[2] A. Corma, Chem. Rev. 97 (1997) 2373.
[3] B. Notari, Adv. Catal. 41 (1996) 253.
[4] S. Dzwigaj, M.J. Peltre, P. Massiani, A. Davidson, M. Che, T. Sen, S. Sivasanker, Chem. Commun. (1998) 87.
[5] (a) S. Dzwigaj, M. Matsuoka, R. Franck, M. Anpo, M. Che, J. Phys. Chem. B 102 (1998) 6309;
(b) S. Dzwigaj, M. Matsuoka, M. Anpo, M. Che, J. Phys. Chem. B 104 (2000) 6012.
[6] S. Dzwigaj, P. Massiani, A. Davidson, M. Che, J. Mol. Catal. 155 (2000) 169.
[7] R. Hajjar, Y. Millot, P.P. Man, M. Che, S. Dzwigaj, J. Phys. Chem. C 112 (2008) 20167.
[8] S. Dzwigaj, El.M. El Malki, M.J. Peltre, P. Massiani, A. Davidson, M. Che, Topics Catal. 11/12 (2000) 379.
[9] S. Dzwigaj, M. Che, Catal. Today, in press, doi:10.1016/j.cattod.2011.01.035.
[10] C.H. Bartholomew, R.J. Farrauto, Fundamentals of Industrial Catalytic Processes, John Wiley & Sons, Inc., 2005.
[11] A.P. Vieira Soares, M. Farinha Portela, A. Kiennemann, Chem. Rev. 47 (2005) 125.
[12] C. Louis, J.M. Tatibouët, M. Che, J. Catal. 109 (1988) 354.
[13] J.M. Tatibouët, M. Che, M. Amirouche, M. Fournier, C. Rocchiccioli-Deltcheff, J. Chem. Soc., Chem. Commun. (1988) 1260.
[14] J.M. Tatibouët, Appl. Catal. A 148 (1997) 213.
[15] R.Z. Khaliullin, A.T. Bell, J. Phys. Chem. B 106 (2002) 7832.
[16] M. Trejda, J. Kujawa, M. Ziolek, Catal. Lett. 108 (2006) 141.
[17] I. Sobczak, N. Kieronczyk, M. Trejda, M. Ziolek, Catal. Today 139 (2008) 188.
[18] C. Louis, M. Che, M. Anpo, J. Catal. 141 (1993) 453.
[19] D. Masure, P. Chaquin, C. Louis, M. Che, M. Fournier, J. Catal. 119 (1989) 415.
[20] L.J. Burcham, I.E. Wachs, Catal. Today 49 (1999) 467.
[21] X. Gao, I.E. Wachs, M.S. Wong, J.Y. Ying, J. Catal. 203 (2001) 18.
[22] C.F. Baes, R.E. Mesmer, in: The Hydrolysis of Cations, John Wiley and Sons, New York, 1976, p. 210.
[23] F. Tielens, M. Calatayud, S. Dzwigaj, M. Che, Micropor. Mesopor. Mater. 119 (2009) 137.
[24] E. Bourgeat-Lami, F. Fajula, D. Anglerot, T. des Courières, Micropor. Mater. 1 (1993) 237.
[25] C. Pazé, A. Zecchina, S. Spera, A. Cosma, E. Merlo, G. Spano, G. Girotti, Phys. Chem. Chem. Phys. 1 (1999) 2627.
[26] L.W. Beck, J.F. Haw, J. Phys. Chem. 99 (1995) 1076.
[27] L.W. Beck, J.L. White, J.F. Haw, J. Am. Chem. Soc. 116 (1994) 9654.
[28] A. Zecchina, S. Bordiga, G. Spoto, L. Marchese, G. Petrini, G. Leofanti, M. Padovan, J. Phys. Chem. 96 (1992) 4991.
[29] G.I. Woolery, L.B. Alemany, R.M. Dessau, A.W. Chester, Zeolites 6 (1986) 14.
[30] G.E. Maciel, P.D. Ellis, in: A.T. Bell, A. Pines (Eds.), NMR Techniques in Catalysis, Dekker, New York, 1994, p. 231.
[31] C.K. Jørgensen, in: Absorption Spectra and Chemical Bonding in Complexes, Pergamon, New York, 1962, p. 309.
[32] Z. Luan, J. Xu, H. He, J. Klinowski, L. Kevan, J. Phys. Chem. 100 (1996) 19595.
[33] G. Centi, S. Perathoner, F. Trifiro, A. Aboukais, C.F. Aïssi, M. Guelton, J. Phys. Chem. 96 (1992) 2617.
[34] J. Kornatowski, B. Wichterlova, M. Rozwadowski, W.H. Baur, Stud. Surf. Sci. Catal. 84 (1994) 117.
[35] B.I. Whittington, J.R. Anderson, J. Phys. Chem. 97 (1993) 1032.
[36] B. Sulikowski, Z. Olejniczak, E. Wloch, J. Rakoczy, R.X. Valenzuela, V. Cortés Corberan, Appl. Catal. A 232 (2002) 189.
[37] Z. Sojka, M. Che, J. Phys. Chem. 99 (1995) 5418.
[38] G. Busca, A.S. Elmi, P. Forzatti, J. Phys. Chem. 91 (1987) 5263.
[39] C. Rocchiccioli-Deltcheff, M. Amirouche, M. Che, J.M. Tatibouët, M. Fournier, J. Catal. 125 (1990) 292.
[40] C. Rocchiccioli-Deltcheff, M. Amirouche, G. Hervé, M. Fournier, M. Che, J.M. Tatibouët, J. Catal. 126 (1990) 591.
[41] K. Brückman, J.M. Tatibouët, M. Che, E. Serwicka, J. Haber, J. Catal. 139 (1993) 455.
[42] K. Brückman, M. Che, J. Haber, J.M. Tatibouët, Catal. Lett. 25 (1994) 225.
[43] M. Che, C. Louis, J.M. Tatibouët, Polyhedron 5 (1986) 123.